




The bivariate distribution of amyloid- β and tau: relationship with established neurocognitive clinical syndromes

 Clifford R. Jack, Jr,¹ Heather J. Wiste,²  Hugo Botha,³ Stephen D. Weigand,² Terry M. Therneau,² David S. Knopman,³ Jonathan Graff-Radford,³ David T. Jones,^{1,3} Tanis J. Ferman,⁴  Bradley F. Boeve,³ Kejal Kantarci,¹ Val J. Lowe,⁵ Prashanthi Vemuri,¹ Michelle M. Mielke,⁶ Julie A. Fields,⁷ Mary M. Machulda,⁷ Christopher G. Schwarz,¹ Matthew L. Senjem,¹ Jeffrey L. Gunter¹ and Ronald C. Petersen³

See Gordon and Tijms (doi:10.1093/brain/awz278) for a scientific commentary on this article.

Large phenotypically diverse research cohorts with both amyloid and tau PET have only recently come into existence. Our objective was to determine relationships between the bivariate distribution of amyloid- β and tau on PET and established clinical syndromes that are relevant to cognitive ageing and dementia. All individuals in this study were enrolled in the Mayo Clinic Study of Aging, a longitudinal population-based study of cognitive ageing, or the Mayo Alzheimer Disease Research Center, a longitudinal study of individuals recruited from clinical practice. We studied 1343 participants who had amyloid PET and tau PET from 2 April 2015 to 3 May 2019, and met criteria for membership in one of five clinical diagnostic groups: cognitively unimpaired, mild cognitive impairment, frontotemporal dementia, probable dementia with Lewy bodies, and Alzheimer clinical syndrome. We examined these clinical groups in relation to the bivariate distribution of amyloid and tau PET values. Individuals were grouped into amyloid (A)/tau (T) quadrants based on previously established abnormality cut points of standardized uptake value ratio 1.48 (A) and 1.33 (T). Individual participants largely fell into one of three amyloid/tau quadrants: low amyloid and low tau (A–T–), high amyloid and low tau (A+T–), or high amyloid and high tau (A+T+). Seventy per cent of cognitively unimpaired and 74% of FTD participants fell into the A–T– quadrant. Participants with mild cognitive impairment spanned the A–T– (42%), A+T– (28%), and A+T+ (27%) quadrants. Probable dementia with Lewy body participants spanned the A–T– (38%) and A+T– (44%) quadrants. Most (89%) participants with Alzheimer clinical syndrome fell into the A+T+ quadrant. These data support several conclusions. First, among 1343 participants, abnormal tau PET rarely occurred in the absence of abnormal amyloid PET, but the reverse was common. Thus, with rare exceptions, amyloidosis appears to be required for high levels of 3R/4R tau deposition. Second, abnormal amyloid PET is compatible with normal cognition but highly abnormal tau PET is not. These two conclusions support a dynamic biomarker model in which Alzheimer's disease is characterized first by the appearance of amyloidosis and later by tauopathy, with tauopathy being the proteinopathy associated with clinical symptoms. Third, bivariate amyloid and tau PET relationships differed across clinical groups and thus have a role for clarifying the aetiologies underlying neurocognitive clinical syndromes.

- 1 Department of Radiology, Mayo Clinic, Rochester, MN, USA
- 2 Department of Health Sciences Research, Mayo Clinic, Rochester, MN, USA
- 3 Department of Neurology, Mayo Clinic, Rochester, MN, USA
- 4 Department of Psychology, Mayo Clinic, Jacksonville, FL, USA
- 5 Department of Nuclear Medicine, Mayo Clinic, Rochester, MN, USA
- 6 Department of Epidemiology, Mayo Clinic, Rochester, MN, USA
- 7 Department of Psychiatry and Psychology, Mayo Clinic, Rochester, MN, USA

Received May 23, 2019. Revised June 26, 2019. Accepted July 7, 2019. Advance Access publication September 9, 2019

© The Author(s) (2019). Published by Oxford University Press on behalf of the Guarantors of Brain.

This is an Open Access article distributed under the terms of the Creative Commons Attribution Non-Commercial License (<http://creativecommons.org/licenses/by-nc/4.0/>), which permits non-commercial re-use, distribution, and reproduction in any medium, provided the original work is properly cited. For commercial re-use, please contact journals.permissions@oup.com

Correspondence to: Clifford R. Jack, Jr, MD
200 First St. SW
Rochester, MN 55905, USA
E-mail: jack.clifford@mayo.edu

Keywords: amyloid PET; tau PET; Alzheimer's disease; dementia with Lewy bodies; frontotemporal dementia

Abbreviations: ADRC = Mayo Alzheimer Disease Research Center; AlzCS = Alzheimer clinical syndrome; DLB = dementia with Lewy bodies; FTD = frontotemporal dementia; MCI = mild cognitive impairment; MCSA = Mayo Clinic Study of Aging; SUVR = standardized uptake value ratio

Introduction

The first successful amyloid PET ligand was reported 15 years ago (Klunk *et al.*, 2004), and over the past decade and a half investigators in the ageing and dementia field have thoroughly examined relationships between amyloid PET and various clinical presentations (Rabinovici *et al.*, 2008; Nordberg *et al.*, 2013; Villemagne *et al.*, 2013; Ossenkoppele *et al.*, 2015; Bilgel *et al.*, 2018; Buckley *et al.*, 2018; Gordon *et al.*, 2018; Jansen *et al.*, 2018; Lim *et al.*, 2018; Lopez *et al.*, 2018; Leuzy *et al.*, 2019; Timmers *et al.*, 2019). More recently, relationships between tau PET and various clinical presentations have also been reported (Cho *et al.*, 2016b; Johnson *et al.*, 2016; Ossenkoppele *et al.*, 2016, 2018; Scholl *et al.*, 2016; Chiotis *et al.*, 2018; Maass *et al.*, 2018; Gordon *et al.*, 2019; Sperling *et al.*, 2019). Because tau PET was only recently introduced into the academic community (Chien *et al.*, 2013), very large phenotypically diverse research cohorts with both amyloid and tau PET have only recently come into existence. Our main objective was to determine relationships between the bivariate distribution of amyloid- β and tau on PET and established clinical syndromes relevant to cognitive ageing and dementia: cognitively unimpaired, mild cognitive impairment (MCI), frontotemporal dementia (FTD), probable dementia with Lewy bodies (DLB), and Alzheimer clinical syndrome (AlzCS).

Materials and methods

Enrolment and clinical characterization

This study was approved by the Mayo Clinic and Olmsted Medical Center Institutional Review Boards. Written informed consent was obtained from all participants and in the case of persons with cognitive impairment sufficient to interfere with capacity, from a close family member.

All individuals in this study were enrolled in one of two studies. The Mayo Clinic Study of Aging (MCSA) is a longitudinal population-based study of cognitive ageing among a stratified random sample of a geographically defined population (Roberts *et al.*, 2008). Residents of Olmsted County, Minnesota, USA aged 30–89 years old were enumerated using the medical records-linkage system of the Rochester Epidemiology Project (St Sauver *et al.*, 2012). From this

sampling frame, individuals were randomly selected by 10-year age and sex strata such that males and females were represented equally. All individuals without a medical contraindication were invited to participate in imaging studies. The Mayo Alzheimer Disease Research Center (ADRC) is a longitudinal research study of individuals recruited from clinical practice.

Evaluations included a medical history review and interview with the participant and a study partner, a neurological examination by a physician; and a neuropsychological examination (Roberts *et al.*, 2008). Participants were assigned a diagnosis of cognitively unimpaired (defined as not MCI or dementia), MCI (Petersen, 2004), or dementia (American Psychiatric Association, 1994) using established criteria. Among individuals with dementia, syndromic diagnoses followed established criteria for FTD syndromes (Gorno-Tempini *et al.*, 2011; Rascovsky *et al.*, 2011), probable DLB (McKeith *et al.*, 2017), and AlzCS (McKhann *et al.*, 1984, 2011; Jack *et al.*, 2018). The AlzCS group included individuals with a classic amnesic phenotype who would meet clinical criteria for probable Alzheimer's disease (McKhann *et al.*, 1984, 2011), as well as established atypical Alzheimer's disease phenotypes (i.e. language, visuospatial, and dysexecutive) (Wolk *et al.*, 2012; Jones *et al.*, 2017). Clinical diagnoses were always made blinded to PET results in the MCSA; however, this was not always the case for ADRC participants.

The study sample consisted of 1343 participants who met the following criteria (Supplementary Fig. 1). For inclusion an individual must have been a participant in the MCSA or ADRC, had amyloid PET, tau PET, and MRI (MR is used for PET quantification) from 2 April 2015 to 3 May 2019, and have met criteria above for membership in one of the five clinical diagnostic groups described above. We excluded individuals who: (i) were cognitively impaired but did not meet established criteria for one of the five syndromic diagnostic groups above; (ii) could not be confidently labelled either cognitively impaired or unimpaired; (iii) had imaging studies that were inadequate for technical reasons; and (iv) were members of families with known mutations. We used data from the first imaging session for individuals with serial imaging.

Imaging methods

Amyloid PET imaging was performed with Pittsburgh Compound B (PIB) (Klunk *et al.*, 2004) and tau PET with flortaucipir (Chien *et al.*, 2013). Amyloid and tau PET standardized uptake value ratios (SUVRs) were formed by normalizing composite multi-region target regions of interest to the cerebellar crus grey matter (Jack *et al.*, 2017). The amyloid PET target meta-region of interest included the prefrontal, orbitofrontal, parietal, temporal, anterior and posterior

cingulate, and the precuneus (Jack *et al.*, 2017). The tau PET target meta-region of interest used in our primary analysis included the amygdala, entorhinal cortex, fusiform, parahippocampal, and inferior temporal and middle temporal gyri (Jack *et al.*, 2017). As a *post hoc* sensitivity analysis, we examined three alternative tau PET reporter regions of interest highlighted in recent publications (Cho *et al.*, 2016a; Johnson *et al.*, 2016; Scholl *et al.*, 2016; Maass *et al.*, 2017; Mishra *et al.*, 2017; Pontecorvo *et al.*, 2017a; Lowe *et al.*, 2018). They were: (i) entorhinal cortex; (ii) inferior temporal gyrus; and (iii) a lateral parietal meta-region of interest composed of the angular, supramarginal, and inferior parietal regions of interest. PET data were not partial volume corrected. MRI was performed at 3 T and was used in the PET data processing pipeline, described in previous work (Schwarz *et al.*, 2019).

Statistical methods

Our main objective was to determine relationships between the bivariate distribution of amyloid- β and tau on PET and established clinical syndromes. To clearly illustrate this, the bivariate distribution of tau and amyloid PET SUVR values over the study sample was segmented into quadrants using cut points based on previously published research (Jack *et al.*, 2017). The amyloid PET cut point was the SUVR value 1.48 (centiloid 22; Klunk *et al.*, 2015), beyond which rates of amyloid PET reliably increased (Jack *et al.*, 2017). The cut point for tau PET (SUVR 1.33) was the value that most accurately discriminated between cognitively impaired individuals with abnormal amyloid and age-matched cognitively unimpaired individuals with normal amyloid (Jack *et al.*, 2017). Previously, we have described both lenient and conservative (i.e. labels fewer people abnormal) cut points for tau PET (Jack *et al.*, 2017) and used the latter here because the questions pertain to aetiological diagnoses in impaired individuals.

In addition to the above, a cluster analysis of the amyloid and tau PET SUVR values was performed using a model-based clustering approach (Banfield and Raftery, 1993; Scrucca *et al.*, 2016). The model treats the data as a mixture of Gaussian densities; it estimates the optimal number of clusters along with the centre and shape of each cluster by optimizing the Bayesian information criterion. An additional ‘diffuse’ cluster was added to the model that covers the entire range of amyloid and tau values, this serves to make the primary results resistant to any outlier points by assigning them to the random background (Banfield and Raftery, 1993).

Data availability

The Mayo Clinic Study of Aging and Alzheimers Disease Research Center make data available to qualified researchers upon reasonable request.

Results

Study participants

The majority of individuals in this study were cognitively unimpaired and most of these were participants in the MCSA (Table 1). MCI participants were split approximately evenly between the MCSA and ADRC. Nearly all

individuals with dementia were participants in the ADRC. The probable DLB group had the highest proportion of males and the AlzCS group had the highest proportion of *APOE* $\epsilon 4$ carriers. Within the FTD group, 14 (61%) were diagnosed as behavioural variant FTD, seven (30%) as semantic dementia, one (4%) as progressive non-fluent aphasia, and one (4%) as progressive associative agnosia (Gorno-Tempini *et al.*, 2011; Rascovsky *et al.*, 2011).

Primary analysis: clinical diagnostic groups within the bivariate amyloid and tau PET distribution

Figure 1 shows the bivariate amyloid and tau PET distribution with individual points colour-coded to represent the five clinical diagnostic groups. Despite a positive rank correlation between amyloid and tau PET overall ($\rho = 0.57$, $P < 0.001$), rather than showing a prototypical ellipsoid bivariate relationship, few individuals were present in the upper left region. The marginal histograms for amyloid and tau in Fig. 1 illustrate that the distribution of amyloid PET values in the ADRC were bimodal, while in the MCSA they were unimodal with a long right tail even when plotted on log scale. The distribution of tau PET values in the ADRC was unimodal with a long right tail but was unimodal and roughly Gaussian in the MCSA.

In Fig. 2A we illustrate results of our clustering procedure based on a three-cluster model with data points coloured to indicate cluster. Black data points were identified as not consistent with any of the three clusters. Ellipses represent the centre 50% of data for each cluster distribution. Three clusters were chosen as optimal based on Bayesian information criterion of -969 , -1338 , -1405 , -1401 , and -1367 for one, two, three, four, and five clusters, respectively. We also superimpose previously established amyloid and tau PET cut points that segregate the bivariate distribution into four quadrants: normal amyloid and normal tau (A–T–), abnormal amyloid and normal tau (A+T–), abnormal amyloid and abnormal tau (A+T+), and normal amyloid and abnormal tau (A–T+). The clustering also suggested a quadrant-based interpretation that is similar to the cut point based quadrants. For both methods few individuals were in the upper left quadrant.

The cluster ellipses and standard cut points are shown again in Fig. 2B with the bivariate medians (centroids) of the clinical groups added. The centroids of the cognitively unimpaired and FTD groups were located in the A–T– quadrant and within what we call the low-low cluster ellipse. The AlzCS centroid was in the A+T+ quadrant and what we call the high-high cluster ellipse. The probable DLB centroid fell in the A+T– quadrant and within what we call the high-low cluster ellipse. The MCI centroid was on the border between the A–T– and A+T– quadrants and situated between the ellipses for the low-low and high-low clusters.

Figure 3 shows the proportion of individuals in each of the five clinical groups that fall into the cut point based and cluster

Table 1 Demographic characteristics of study participants

Characteristic	CU	MCI	AlzCS	DLB	FTD
Number of subjects	976	182	123	39	23
Study, <i>n</i> (%)					
MCSA	903 (93)	92 (51)	8 (7)	3 (8)	0 (0)
ADRC ^a	73 (7)	90 (49)	115 (93)	36 (92)	23 (100)
Age, years					
Median (IQR)	68 (57, 77)	74 (67, 81)	69 (61, 77)	70 (66, 77)	65 (58, 69)
Min, Max	30, 98	44, 94	52, 89	51, 88	49, 73
Male sex, <i>n</i> (%)	526 (54)	117 (64)	51 (41)	31 (79)	14 (61)
Education, years					
Median (IQR)	16 (13, 17)	16 (12, 18)	16 (12, 16)	15 (14, 18)	16 (15, 18)
Min, Max	6, 20	0, 24	8, 25	7, 20	12, 21
APOE ε4 carrier, <i>n</i> (%)	258 (28)	66 (39)	74 (69)	12 (44)	5 (29)
Short Test of Mental Status score					
Median (IQR)	37 (35, 38)	33 (30, 35)	24 (19, 29)	29 (24, 32)	27 (23, 32)
Min, Max	26, 38	22, 38	4, 36	8, 35	20, 36
Amyloid PET SUVR					
Median (IQR)	1.38 (1.31, 1.51)	1.53 (1.36, 2.25)	2.47 (2.20, 2.71)	1.68 (1.37, 2.32)	1.36 (1.26, 1.45)
Min, Max	1.10, 3.63	1.15, 3.41	1.28, 3.41	1.25, 3.00	1.16, 2.16
Centiloid					
Median (IQR)	13 (6, 24)	26 (11, 90)	110 (86, 131)	39 (12, 96)	11 (2, 19)
Min, Max	−13, 212	−8, 193	4, 193	1, 157	−7, 82
<i>n</i> (%) abnormal ^b	282 (29)	101 (55)	119 (97)	23 (59)	4 (17)
Tau PET, SUVR					
Median (IQR)	1.18 (1.12, 1.23)	1.25 (1.18, 1.38)	1.97 (1.60, 2.29)	1.25 (1.17, 1.31)	1.23 (1.20, 1.31)
Min, Max	0.87, 1.75	0.91, 2.49	1.09, 3.27	1.05, 2.22	1.10, 1.40
<i>n</i> (%) abnormal ^c	54 (6)	55 (30)	109 (89)	7 (18)	4 (17)

CU = cognitively unimpaired.

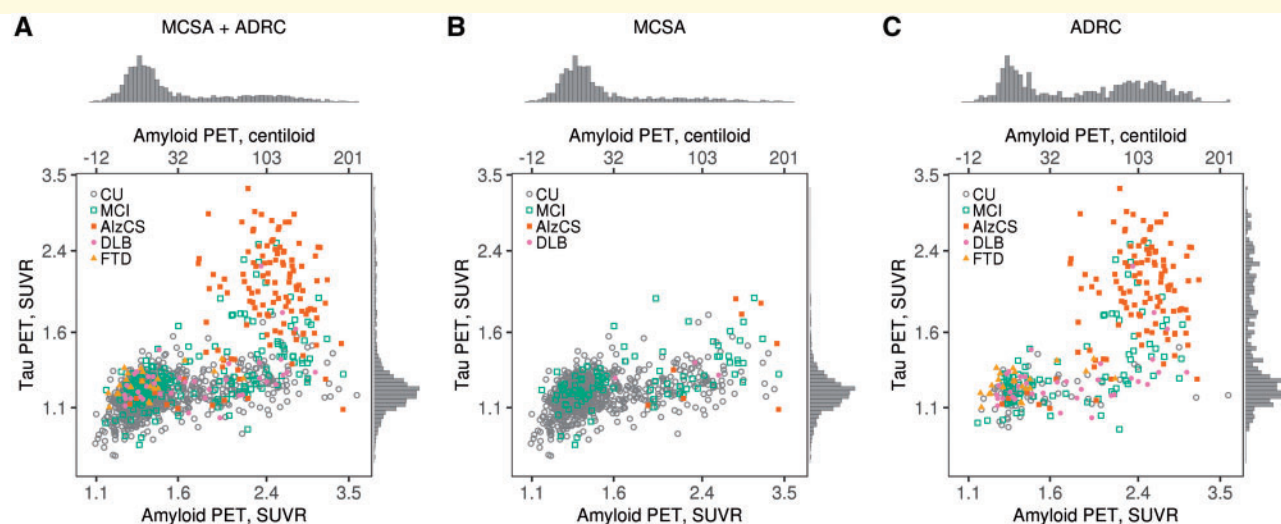
^aADRC includes 12 participants co-enrolled in the Advancing Research and Treatment for Frontotemporal Lobar Degeneration Project I Study (one MCI, two AlzCS, nine FTD).^bAmyloid PET abnormality is defined as ≥ 1.48 SUVR.^cTau PET abnormality is defined as ≥ 1.33 SUVR.

Figure 1 Amyloid and tau PET distributions by clinical group overall and within study. Scatter plots of tau PET SUVR versus amyloid PET SUVR among all individuals combined (**A**) and separately among individuals in the MCSA (**B**) and ADRC (**C**). Tau PET and amyloid PET values are in SUVR units but the data is plotted on log scale, which accounts for the uneven spacing. Points are coloured by clinical diagnosis. Histograms in the margins show the distributions of tau PET SUVR (*right*) and amyloid PET SUVR (*top*). Axis labels on the *top* represent amyloid PET values on a centiloid scale.

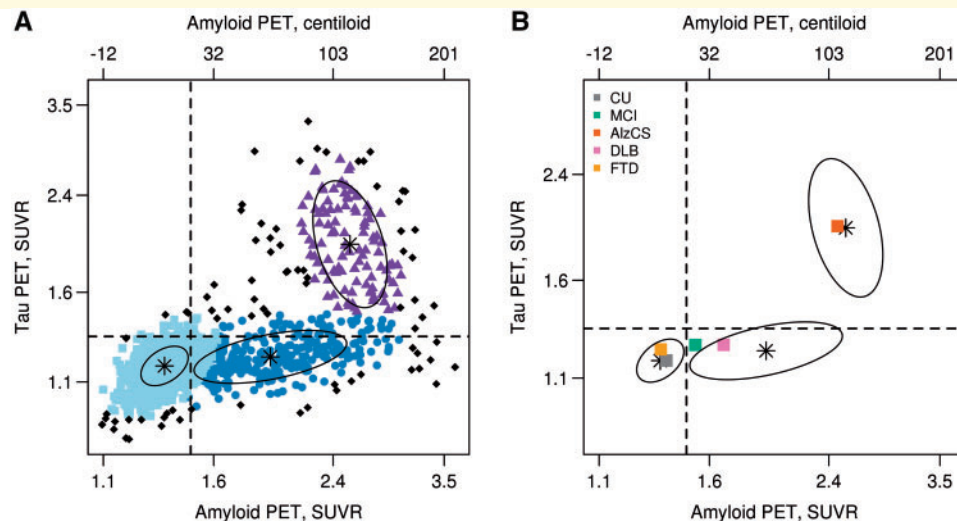


Figure 2 Amyloid and tau PET clusters. Scatterplot of tau PET SUVR versus amyloid PET SUVR with points coloured according to the three-cluster classification from a bivariate mixture model (**A**). Points shown in black represent individuals who were inconsistent with one of the three clusters. The vertical and horizontal lines represent the cut points of 1.48 SUVR for amyloid PET and 1.33 SUVR for tau PET. The ellipses show the centre 50% of the data for the three cluster distributions with a black star indicating the bivariate mean from the clustering. In **B**, these ellipses are shown along with a square for each clinical diagnosis group representing the bivariate median (centroid) of the tau and amyloid distributions. Tau PET and amyloid PET values are in SUVR units but the data is plotted on log scale, which accounts for the uneven spacing. Axis labels on the top represent amyloid PET values on a centiloid scale.

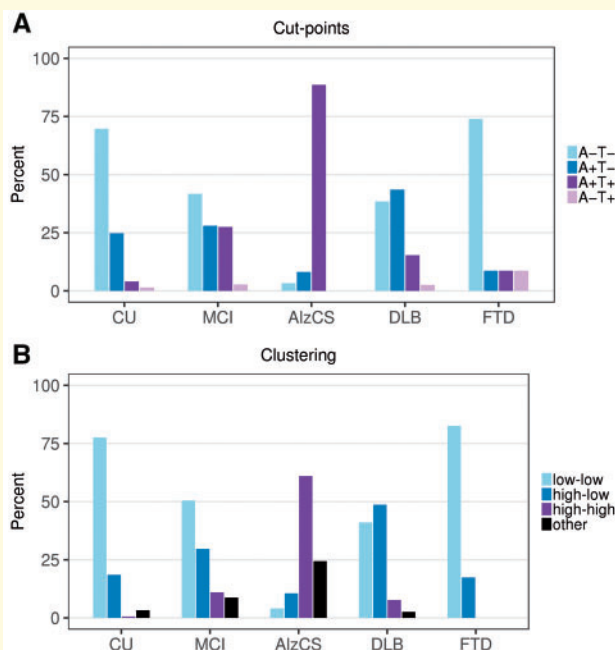


Figure 3 Amyloid and tau PET groups within clinical diagnosis. Per cent of individuals in each quadrant (**A**) or cluster (**B**) within each clinical diagnostic group. (**A**) Percentages according to amyloid and tau PET groupings based on the established cut points of 1.48 SUVR for amyloid PET and 1.33 SUVR for tau PET. (**B**) Percentages according to the bivariate mixture model clusters. These are labelled according to amyloid (low or high) and tau (low or high). Those individuals whose values were inconsistent with one of the three clusters were labelled as other.

based quadrants. Using established cut points (Jack *et al.*, 2017) most cognitively unimpaired individuals fell into either the A-T- (70%) or A+T- (25%) quadrants, but a few were in the A+T+ (4%) and A-T+ (1%) quadrants. Among MCI, 42% were in the A-T- quadrant, 28% in the A+T- quadrant, 27% in the A+T+ quadrant, and only 3% in the A-T+ quadrant. The large majority of AlzCS individuals were in the A+T+ quadrant (89%) but a few were in the A-T- (3%) and A+T- (8%) quadrants. Probable DLB individuals were generally in either the A-T- (38%) or A+T- (44%) quadrants, while the majority of the FTD individuals were in the A-T- quadrant (74%) (Supplementary Table 1). These patterns were similar for the cluster-based quadrants.

Secondary analysis: bivariate amyloid and tau PET distribution by age among unimpaired, MCI, and AlzCS individuals

In Fig. 4 we illustrate the bivariate amyloid and tau PET distribution by age restricted to cognitively unimpaired, MCI and AlzCS participants. In the MCSA, nearly all (97%) individuals under 60 years of age were A-T- while those above 60 fell in each of the A-T- (55%), A+T- (35%), and A+T+ (9%) quadrants. In contrast, younger individuals were more equally present in both the A-T- (46%) and A+T+ (49%) quadrants in the ADRC.

Post hoc sensitivity analyses

In Supplementary Fig. 2 we illustrate correlations between different tau PET reporter regions of interest. The temporal

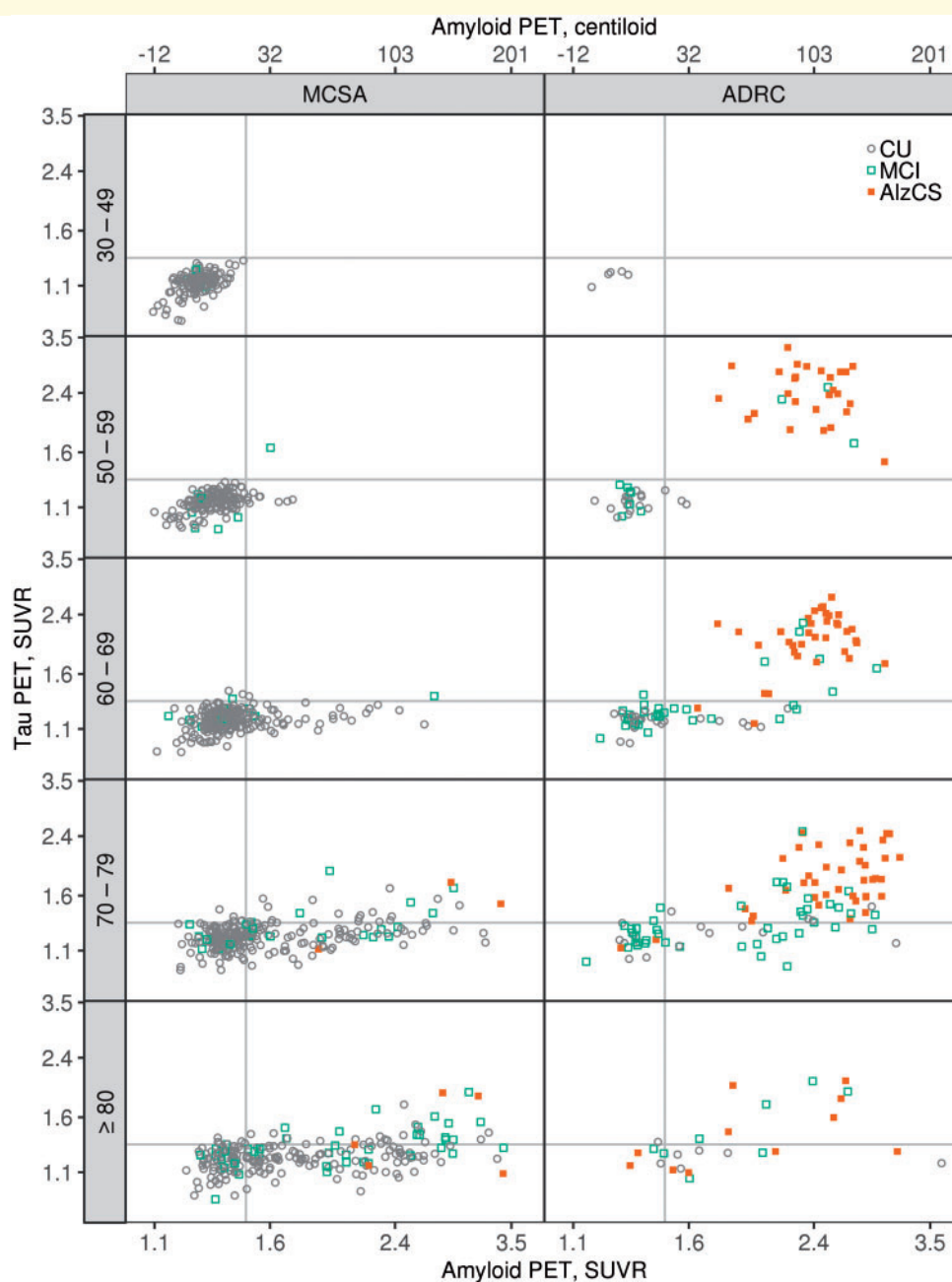


Figure 4 Scatter plots of tau PET SUVR versus amyloid PET SUVR by age groups among cognitively unimpaired (CU), MCI, and AlzCS individuals. MCSA individuals are shown in the left column and ADRC individuals in the right column. The vertical and horizontal lines represent the cut points of 1.48 SUVR for amyloid PET and 1.33 SUVR for tau PET. Points are coloured by clinical diagnosis. Tau PET and amyloid PET values are in SUVR units but the data is plotted on a log scale, which accounts for the uneven spacing. Axis labels on the top of the columns represent amyloid PET values on a centiloid scale.

meta-region of interest used in the primary analysis was highly correlated with the entorhinal cortex ($\rho = 0.86$), inferior temporal ($\rho = 0.99$), and lateral parietal ($\rho = 0.91$) regions of interest. The entorhinal cortex had a ceiling effect relative to the other regions of interest. Figure 5 illustrates the bivariate amyloid and tau PET to clinical diagnostic group relationships for these three alternative tau PET regions of interest. Except for the ceiling

effect in the entorhinal cortex, the bivariate distributions were similar to that of the temporal meta-region of interest.

Discussion

The clinical diagnoses in this sample were based on well-defined syndromic presentations. Each syndrome in turn is

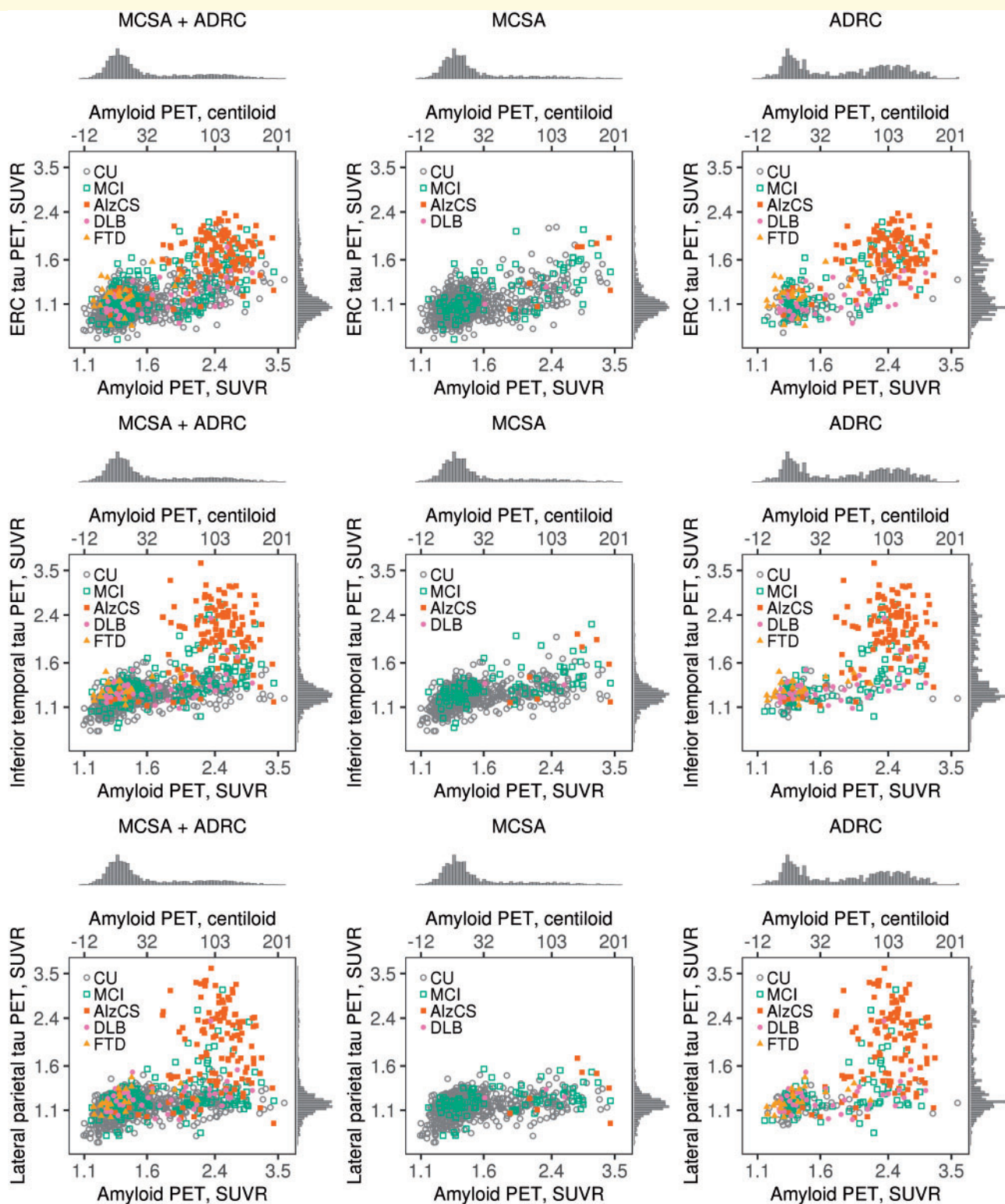


Figure 5 Scatter plots of tau PET SUVR versus amyloid PET SUVR among all individuals combined and separately among individuals in the MCSA and ADRC for three alternative tau PET regions of interest. Points are coloured by clinical diagnosis. Histograms in the margins show the distributions of tau PET SUVR (right) and amyloid PET SUVR (top). Axis labels on the top of each plot represent amyloid PET values on a centiloid scale. Tau PET and amyloid PET values are in SUVR units but the data is plotted on a log scale, which accounts for the uneven spacing.

linked with an expected aetiology. For example, the expected aetiology in probable DLB is α -synuclein pathology, and in AlzCS it is Alzheimer's disease. Patient management decisions are driven by the aetiologies that physicians suspect underlie specific syndromic presentations (Pontecorvo *et al.*, 2017b; de Wilde *et al.*, 2018; Rabinovici *et al.*, 2019). However, a clinical syndrome is often an imperfect indicator of underlying aetiology (Beach *et al.*, 2012; Jagust *et al.*, 2019). Our data illustrate that the combination of amyloid and tau PET provides useful information about the aetiology underlying various common neurocognitive syndromes at the individual patient level.

The A+T+ biomarker profile identifies Alzheimer's disease *in vivo* in the NIA-AA research framework (Jack *et al.*, 2018) and about 9 in 10 AlzCS participants in this study were A+T+. The 8% (Supplementary Table 1) of AlzCS participants who were A+T– would be labelled Alzheimer pathological change in the NIA-AA research framework (Jack *et al.*, 2018). Low levels of Alzheimer's disease tauopathy that lie below the tau PET detection threshold could account for a portion of the symptoms in A+T– individuals (Knopman *et al.*, 2019). However, the dementia is likely due, at least in part, to one or more ageing-related non-Alzheimer disorders, e.g. TDP-43 (recently labelled LATE disease; Nelson *et al.*, 2019) with or without hippocampal sclerosis, α -synuclein deposits, argyrophilic grain disease, or cerebrovascular disease (particularly microscopic cerebral infarctions) (Schneider *et al.*, 2007; Sonnen *et al.*, 2007; Nelson *et al.*, 2011; Kawas *et al.*, 2015; Botha *et al.*, 2018a, b; Petersen, 2018). In A–T– individuals diagnosed clinically as AlzCS, symptoms are almost certainly due to one or more of the aforementioned non-Alzheimer disorders.

Probable DLB participants were distributed between the A–T– and A+T– quadrants (Fig. 3). The A–T– individuals likely represent more pure α -synuclein pathology while the A+T– individuals represent α -synuclein pathology plus Alzheimer pathological change (Walker *et al.*, 2015; Irwin *et al.*, 2017; Coughlin *et al.*, 2019). Because α -synuclein pathology and Alzheimer's disease often coexist, patients may present with overlapping clinical features (Walker *et al.*, 2015). The combination of amyloid and tau PET may aid the clinician by indicating the status of a patient within the Alzheimer continuum and thereby informing on aetiologies underlying symptoms. Many probable DLB patients also meet neuropathological criteria for Alzheimer's disease at autopsy (Walker *et al.*, 2015; Irwin *et al.*, 2017) and therefore a higher number of A+T+ probable DLB patients might have been expected in our study. However, flortaucipir retention is greater in AlzCS than in probable DLB in most areas of the brain (Gomperts *et al.*, 2016; Kantarci *et al.*, 2017) and when tau is present in pathologically confirmed DLB, the pathological burden is usually lower than it is in Alzheimer's disease (Walker *et al.*, 2015; Coughlin *et al.*, 2019). We used a conservative cut point for tau PET (Jack *et al.*, 2017) here, and the tau burden in mildly affected probable DLB (median Short Test

of Mental Status score 29, Table 1) patients may have fallen below this cut point.

Most FTD participants were A–T–, which was anticipated as these individuals are not considered to lie in the Alzheimer continuum (Fig. 3). Four, however, had high amyloid PET levels. All four were over age 60 and may have had fronto-temporal lobar degeneration plus Alzheimer continuum pathology (Jack *et al.*, 2018). Discrimination between fronto-temporal lobar degeneration and Alzheimer's disease on clinical grounds can occasionally be difficult and this distinction may be aided by joint amyloid and tau PET. Flortaucipir was developed to bind to the 3R/4R form of pathological tau that characterizes Alzheimer's disease (Chien *et al.*, 2013; Lowe *et al.*, 2016; Lemoine *et al.*, 2017; Marquie *et al.*, 2017). If a tau PET ligand is developed that is sensitive to the tau deposits in primary tauopathies, then many patients in the FTD spectrum would likely exhibit an A–T+ biomarker profile when imaged with such a ligand.

MCI participants were distributed across the A–T–, A+T–, and A+T+ quadrants (Fig. 3). This reflects the aetiological heterogeneity of the MCI syndrome (Markesbery *et al.*, 2006). A+T+ and A+T– individuals are considered to lie within the Alzheimer continuum (Jack *et al.*, 2018) and aetiologies underlying cognitive impairment in these participants are likely similar to those discussed above for AlzCS individuals (Forsberg *et al.*, 2010). A–T– MCI participants may have non-Alzheimer neuropathology or non-degenerative causes for impairment (e.g. sleep disorders, depression, cerebrovascular disease) (Wisse *et al.*, 2015; Landau *et al.*, 2016) and the A–T– biomarker profile suggests excluding Alzheimer's disease as a likely aetiology. The potential value of these biomarkers in patient management is evident. Physicians may be likely to prescribe Alzheimer's disease medications for an A+T+ MCI patient, but unlikely to prescribe these medications for a patient with the same syndromic presentation but who is A–T– (Pontecorvo *et al.*, 2017b; Rabinovici *et al.*, 2019).

Among cognitively unimpaired participants, 70% were A–T– and 25% were A+T–. While some cognitively unimpaired individuals had amyloid PET values in the same range as AlzCS, none had tau PET values in the AlzCS range. Further, the few cognitively unimpaired individuals with tau PET values above the tau PET cut point had values that were close to the normal/abnormal cut point (Fig. 4). This suggests that high levels of amyloid are compatible with unimpaired cognitive status while high levels of tau are not, a finding that is consistent with prior evidence that **cognitive impairment in Alzheimer's disease is more closely linked to tau than amyloid- β** (Arriagada *et al.*, 1992; Gomez-Isla *et al.*, 1997; Bennett *et al.*, 2004; Nelson *et al.*, 2012; Ossenkoppele *et al.*, 2016).

Which biomarker abnormality appears first, amyloid versus tau, has been a source of **controversy** in the Alzheimer field. Because earlier events can cause later events but not the reverse, temporal ordering of biomarkers has likewise been linked to discussion of cause and effect.

Our data are cross-sectional and cannot prove specific claims about temporal evolution of biomarkers or cause and effect; however, the prevalence of various amyloid and tau profiles in this large series of participants can inform on the ‘plausibility’ of different possible temporal evolution patterns. Every individual begins life cognitively unimpaired and A–T– (lower left quadrant) and the large majority of AlzCS individuals are A+T+ (upper right quadrant) (Figs 3 and 4). Therefore every A+T+ AlzCS individual had to follow one of the following transition pathways: (i) A–T– to A+T– to A+T+; (ii) A–T– to A–T+ to A+T+; or (iii) from A–T– directly to A+T+. The near absence of individuals in the A–T+ quadrant, along with the observation that all tau PET values in that quadrant lie close to the cut point, makes the second pathway very unlikely. The clear gap in data points along the middle of the 45° diagonal line makes the last option unlikely as well. The placement of clinical group centroids on the tau versus amyloid plot (Fig. 2B) couples the well-established clinical progression of cognitively unimpaired to MCI to AlzCS with a parallel pathway from A–T– to A+T– to A+T+. Finally, Fig. 4 illustrates the bivariate amyloid and tau PET distribution for different ages among cognitively unimpaired, MCI, and AlzCS participants. The clear trend is progression from A–T– to A+T– with age in many participants, with some individuals reaching A+T+. In aggregate these data lead to the conclusion that the typical pathway within the Alzheimer aetiological continuum from cognitively unimpaired to MCI to AlzCS is likely paralleled by transitions from A–T– to A+T– to A+T+. When combined with the evidence suggesting that high levels of amyloid are compatible with unimpaired cognitive status while high levels of tau are not, our data supports the position that within the Alzheimer continuum it is the transition from A+T– to A+T+ that is associated with onset of severe cognitive symptoms. Our data along with that from other studies (Arriagada *et al.*, 1992; Ingelsson *et al.*, 2004; Bateman *et al.*, 2012; Benzinger *et al.*, 2013; Xiong *et al.*, 2016; Leal *et al.*, 2018; Hanseeuw *et al.*, 2019) support a dynamic biomarker model (Jack *et al.*, 2010, 2013) in which amyloidosis promotes or is permissive for the spread of tauopathy and it is the latter proteinopathy that is associated with cognitive symptoms.

The distributions of tau PET values using different reporter regions of interest were highly correlated, particularly the temporal meta-region of interest and the inferior temporal region of interest (Supplementary Fig. 2). Aside from the tau PET ceiling effect in the entorhinal cortex, the bivariate distribution was not greatly different using the entorhinal cortex compared to that seen with other tau reporter regions of interest (Fig. 5), which would imply that the typical progression from A–T– to A+T– to A+T+ is a generalizable conclusion across different choices of tau reporter region of interest.

An important caveat to the conclusion above is that autopsy data show that medial temporal tauopathy likely

precedes neocortical amyloidosis in most people (Braak *et al.*, 2011). Medial/basal temporal lobe tauopathy with no or minimal amyloidosis has been labelled primary age-related tauopathy (Crary *et al.*, 2014), a neuropathological entity attributed to ageing that is distinct from Alzheimer’s disease (Hyman *et al.*, 2012). It is unclear how well flor-taucipir or any currently available tau PET ligand captures low levels of tau pathology in primary age-related tauopathy.

This study has several strengths. First, the large number of participants ($n = 1343$) in this sample lends credibility to the conclusion that a fundamental feature of the biology of Alzheimer’s disease is that amyloidosis is required for extensive 3R/4R tauopathy. Second, all participants were well characterized clinically by the same group of physicians, neuropsychologists, and study coordinators and variability was further reduced by using the same set of magnetic resonance and PET scanners and identical image analysis pipelines. Third, we examined both population-based and clinic-based samples. Population-based samples capture relationships between clinical presentation and imaging that exist commonly in community dwelling individuals, but will not capture more uncommon clinical presentations. In contrast, our clinic-based sample captures less common clinical presentations. When combined, we were able to study the full spectrum of the bivariate amyloid and tau distribution.

This study has several limitations. First, *in vivo* imaging has fundamental limits in detection sensitivity in comparison to direct examination of tissue at autopsy. Sub-threshold levels of both amyloid (Leal *et al.*, 2018) and tau may be clinically relevant. We cannot know in any individual whether or not subthreshold levels of either proteinopathy are present. Second, the findings are specific for the two PET tracers used and could differ somewhat with different amyloid and tau PET tracers. Third, cut points for amyloid PET have been validated against neuropathology (Murray *et al.*, 2015; La Joie *et al.*, 2019). However, because of its more recent development far less autopsy-imaging validation exists for tau PET. Questions about which areas of the brain should be measured and what constitute valid or useful cut points are still under investigation (Cho *et al.*, 2016a; Johnson *et al.*, 2016; Scholl *et al.*, 2016; Villemagne *et al.*, 2016; Maass *et al.*, 2017; Mishra *et al.*, 2017; Pontecorvo *et al.*, 2017a; Lowe *et al.*, 2018). However, the continuous bivariate amyloid and tau PET distributions (Figs 1, 2, 4 and 5) circumvent the limitations of cut points and illustrate that the primary conclusion that very high tau is not seen in the absence of amyloid would not change with different cut points. Fourth, while clinical diagnoses were all made blinded to PET results in the MCSA, this was not always the case for participants in the ADRC (given its clinic-based nature). However, all participants met rigorously defined, established clinical diagnostic criteria that do not require imaging/biomarker information. Fifth, many individuals presenting to the ADRC with AlzCS (a referral clinic sample) are not representative of AlzCS in the community. The former tend to have a younger age of onset and higher

levels of neocortical tau uptake (Ossenkoppele *et al.*, 2016; Lowe *et al.*, 2018). Sixth, perhaps the most significant limitation, is one shared by all research in this field. Currently available biomarkers that are disease-specific do not fully capture the neuropathological complexity of the ageing brain. Non-Alzheimer pathologies, for which no biomarkers presently exist, are highly prevalent in older individuals (most often co-morbidly), and exert significant effects on cognition (Schneider *et al.*, 2007; Sonnen *et al.*, 2007; Nelson *et al.*, 2011; Kawas *et al.*, 2015; Botha *et al.*, 2018a, b; Petersen, 2018). A major need in the field is the development of either imaging or biofluid biomarkers for these common non-Alzheimer neuropathological entities.

Acknowledgements

We thank AVID Radiopharmaceuticals, Inc., for their support in supplying AV-1451 (flortaucipir) precursor, chemistry production advice and oversight, and FDA regulatory cross-filing permission and documentation needed for this work.

Funding

Study funding was provided by the National Institutes of Health, R37 AG011378, RO1 AG041851, R01 AG056366, R01 NS097495, U01 AG06786, R01 AG034676, P50 AG016574; Alexander Family Professorship of Alzheimer's Disease Research; Alzheimer's Association; The GHR Foundation. The funding organizations/sponsors had no role in design and conduct of the study; collection, management, analysis, and interpretation of the data; preparation, review, or approval of the manuscript; and decision to submit the manuscript for publication.

Competing interests

C.R.J. serves as a consultant for Lilly and serves on an independent data monitoring board for Roche but he receives no personal compensation from any commercial entity; receives funding from the NIH and the Alexander Family Alzheimer's Disease Research Professorship of the Mayo Clinic. D.S.K. serves on a Data Safety Monitoring Board for the DIAN study; is an investigator in clinical trials sponsored by Biogen, Lilly Pharmaceuticals, and the University of Southern California; and receives research support from the NIH/NIA. D.T.J. receives funding from the NIH and the Minnesota Partnership for Biotechnology and Medical Genomics. T.J.F. receives support from the Mayo Clinic Dorothy and Harry T. Mangurian Jr. Lewy Body Dementia Program and NIH. B.B.B. has served as an investigator for a clinical trial sponsored by Biogen. He receives royalties from the publication of a book entitled Behavioral Neurology Of Dementia (Cambridge Medicine, 2009, 2017). He serves on the Scientific Advisory Board of

the Tau Consortium. He receives research support from the NIH, the Mayo Clinic Dorothy and Harry T. Mangurian Jr. Lewy Body Dementia Program, and the Little Family Foundation. K.K. serves on the data safety monitoring board for Takeda Global Research and Development Center, Inc.; receives research support from Avid Radiopharmaceuticals and Eli Lilly, and receives funding from NIH and Alzheimer's Drug Discovery Foundation. V.J.L. consults for Bayer Schering Pharma, Piramal Life Sciences, and Merck Research, and receives research support from GE Healthcare, Siemens Molecular Imaging, AVID Radiopharmaceuticals, and the NIH (NIA, NCI). M.M.M. receives research support from the NIH and unrestricted research grants from Biogen and Lundbeck. P.V., J.A.F., J. G-R. and C.G.S. receive funding from the NIH. M.L.S. at the time of manuscript submission, owned shares of the following medical related stocks, unrelated to the current work: Align Technology, Inc., LHC Group, Inc., Mesa Laboratories, Inc., Natus Medical Incorporated, Varex Imaging Corporation. Within the past 3 years, he has owned the following medical related stocks, unrelated to the current work: CRISPR Therapeutics, Gilead Sciences, Inc., Globus Medical Inc., Inovio Biomedical Corp., Ionis Pharmaceuticals, Johnson & Johnson, Medtronic, Inc., Parexel International Corporation. R.C.P. consults for Roche, Inc.; Merck, Inc.; Genentech, Inc.; Biogen, Inc.; Eisai, Inc. and GE Healthcare and receives royalties from Oxford University Press for Mild Cognitive Impairment H.J.W., H.B., S.D.W., T.M.T., J.L.G., and M.M.M. report no competing interests.

Supplementary material

Supplementary material is available at *Brain* online.

References

- American Psychiatric Association. Diagnostic and statistical manual of mental disorders, DSM-IV. 4th edn. Washington, DC: American Psychiatric Association; 1994.
- Arriagada PV, Growdon JH, Hedley-Whyte ET, Hyman BT. Neurofibrillary tangles but not senile plaques parallel duration and severity of Alzheimer's disease. *Neurology* 1992; 42 (3 Pt 1): 631–9.
- Banfield JD, Raftery AE. Model-based Gaussian and non-Gaussian clustering. *Biometrics* 1993; 49: 803–21.
- Bateman RJ, Xiong C, Benzinger TL, Fagan AM, Goate A, Fox NC, et al. Clinical and biomarker changes in dominantly inherited Alzheimer's disease. *N Engl J Med* 2012; 367: 795–804.
- Beach TG, Monsell SE, Phillips LE, Kukull W. Accuracy of the clinical diagnosis of Alzheimer disease at National Institute on Aging Alzheimer Disease Centers, 2005–2010. *J Neuropathol Exp Neurol* 2012; 71: 266–73.
- Bennett DA, Schneider JA, Wilson RS, Bienias JL, Arnold SE. Neurofibrillary tangles mediate the association of amyloid load with clinical Alzheimer disease and level of cognitive function. *Arch Neurol* 2004; 61: 378–84.
- Benzinger TL, Blazey T, Jack CR Jr, Koeppe RA, Su Y, Xiong C, et al. Regional variability of imaging biomarkers in autosomal dominant Alzheimer's disease. *Proc Natl Acad Sci USA* 2013; 110: E4502–9.

- Bilgel M, An Y, Helprey J, Elkins W, Gomez G, Wong DF, et al. Effects of amyloid pathology and neurodegeneration on cognitive change in cognitively normal adults. *Brain* 2018; 141: 2475–85.
- Botha H, Mantyh WG, Graff-Radford J, Machulda MM, Przybelski SA, Wiste HJ, et al. Tau-negative amnesic dementia masquerading as Alzheimer disease dementia. *Neurology* 2018a; 90: e940–6.
- Botha H, Mantyh WG, Murray ME, Knopman DS, Przybelski SA, Wiste HJ, et al. FDG-PET in tau-negative amnesic dementia resembles that of autopsy-proven hippocampal sclerosis. *Brain* 2018b; 141: 1201–17.
- Braak H, Thal DR, Ghebremedhin E, Del Tredici K. Stages of the pathologic process in Alzheimer disease: age categories from 1 to 100 years. *J Neuropathol Exp Neurol* 2011; 70: 960–9.
- Buckley RF, Mormino EC, Amariglio RE, Properzi MJ, Rabin JS, Lim YY, et al. Sex, amyloid, and APOE ϵ 4 and risk of cognitive decline in preclinical Alzheimer's disease: findings from three well-characterized cohorts. *Alzheimer's Dement* 2018; 14: 1193–203.
- Chien DT, Bahri S, Szardenings AK, Walsh JC, Mu F, Su MY, et al. Early clinical PET imaging results with the novel PHF-tau radioligand [F-18]-T807. *J Alzheimers Dis* 2013; 34: 457–68.
- Chiotis K, Saint-Aubert L, Rodriguez-Vieitez E, Leuzy A, Almkvist O, Savitcheva I, et al. Longitudinal changes of tau PET imaging in relation to hypometabolism in prodromal and Alzheimer's disease dementia. *Mol Psychiatry* 2018; 23: 1666–73.
- Cho H, Choi JY, Hwang MS, Kim YJ, Lee HM, Lee HS, et al. In vivo cortical spreading pattern of tau and amyloid in the Alzheimer disease spectrum. *Ann Neurol* 2016a; 80: 247–58.
- Cho H, Choi JY, Hwang MS, Lee JH, Kim YJ, Lee HM, et al. Tau PET in Alzheimer disease and mild cognitive impairment. *Neurology* 2016b; 87: 375–83.
- Coughlin D, Xie SX, Liang M, Williams A, Peterson C, Weintraub D, et al. Cognitive and pathological influences of tau pathology in Lewy body disorders. *Ann Neurol* 2019; 85: 259–71.
- Crary JF, Trojanowski JQ, Schneider JA, Abisambra JF, Abner EL, Alafuzoff I, et al. Primary age-related tauopathy (PART): a common pathology associated with human aging. *Acta Neuropathol* 2014; 128: 755–66.
- de Wilde A, van der Flier WM, Pelkmans W, Bouwman F, Verwer J, Groot C, et al. Association of amyloid positron emission tomography with changes in diagnosis and patient treatment in an unselected memory clinic cohort: the ABIDE project. *JAMA Neurol* 2018; 75: 1062–70.
- Forsberg A, Almkvist O, Engler H, Wall A, Langstrom B, Nordberg A. High PIB retention in Alzheimer's disease is an early event with complex relationship with CSF biomarkers and functional parameters. *Curr Alzheimer Res* 2010; 7: 56–66.
- Gomez-Isla T, Hollister R, West H, Mui S, Growdon JH, Petersen RC, et al. Neuronal loss correlates with but exceeds neurofibrillary tangles in Alzheimer's disease. *Ann Neurol* 1997; 41: 17–24.
- Gomperts SN, Locascio JJ, Makaretz SJ, Schultz A, Caso C, Vasdev N, et al. Tau positron emission tomographic imaging in the Lewy body diseases. *JAMA Neurol* 2016; 73: 1334–41.
- Gordon BA, Blazey TM, Christensen J, Dincer A, Flores S, Keefe S, et al. Tau PET in autosomal dominant Alzheimer's disease: relationship with cognition, dementia and other biomarkers. *Brain* 2019; 142: 1063–76.
- Gordon BA, Blazey TM, Su Y, Hari-Raj A, Dincer A, Flores S, et al. Spatial patterns of neuroimaging biomarker change in individuals from families with autosomal dominant Alzheimer's disease: a longitudinal study. *Lancet Neurol* 2018; 17: 241–50.
- Gorno-Tempini ML, Hillis AE, Weintraub S, Kertesz A, Mendez M, Cappa SF, et al. Classification of primary progressive aphasia and its variants. *Neurology* 2011; 76: 1006–14.
- Hanseuw BJ, Betensky RA, Jacobs HIL, Schultz AP, Sepulcre J, Becker JA, et al. Association of amyloid and tau with cognition in preclinical Alzheimer disease: a longitudinal study. *JAMA Neurol* 2019; 76: 915–24.
- Hyman BT, Phelps CH, Beach TG, Bigio EH, Cairns NJ, Carrillo MC, et al. National Institute on Aging-Alzheimer's Association guidelines for the neuropathologic assessment of Alzheimer's disease. *Alzheimers Dement* 2012; 8: 1–13.
- Ingelsson M, Fukumoto H, Newell KL, Growdon JH, Hedley-Whyte ET, Frosch MP, et al. Early Abeta accumulation and progressive synaptic loss, gliosis, and tangle formation in AD brain. *Neurology* 2004; 62: 925–31.
- Irwin DJ, Grossman M, Weintraub D, Hurtig HI, Duda JE, Xie SX, et al. Neuropathological and genetic correlates of survival and dementia onset in synucleinopathies: a retrospective analysis. *Lancet Neurol* 2017; 16: 55–65.
- Jack CR Jr, Bennett DA, Blennow K, Carrillo MC, Dunn B, Haeberlein SB, et al. NIA-AA research framework: toward a biological definition of Alzheimer's disease. *Alzheimers Dement* 2018; 14: 535–62.
- Jack CR Jr, Knopman DS, Jagust WJ, Petersen RC, Weiner MW, Aisen PS, et al. Tracking pathophysiological processes in Alzheimer's disease: an updated hypothetical model of dynamic biomarkers. *Lancet Neurol* 2013; 12: 207–16.
- Jack CR Jr, Knopman DS, Jagust WJ, Shaw LM, Aisen PS, Weiner MW, et al. Hypothetical model of dynamic biomarkers of the Alzheimer's pathological cascade. *Lancet Neurol* 2010; 9: 119–28.
- Jack CR, Wiste HJ, Weigand SD, Therneau TM, Lowe VJ, Knopman DS, et al. Defining imaging biomarker cut points for brain aging and Alzheimer's disease. *Alzheimers Dement* 2017; 13: 205–16.
- Jagust W, Jack CR Jr, Bennett DA, Blennow K, Haeberlein SB, Holtzman DM, et al. "Alzheimer's disease" is neither "Alzheimer's clinical syndrome" nor "dementia". *Alzheimer's Dement* 2019; 15: 153–7.
- Jansen WJ, Ossenkoppele R, Tijms BM, Fagan AM, Hansson O, Klunk WE, et al. Association of cerebral amyloid-beta aggregation with cognitive functioning in persons without dementia. *JAMA Psychiatry* 2018; 75: 84–95.
- Johnson KA, Shultz A, Betensky RA, Becker JA, Sepulcre J, Rentz DM, et al. Tau positron emission tomographic imaging in aging and early Alzheimer's disease. *Ann Neurol* 2016; 79: 110–9.
- Jones DT, Graff-Radford J, Lowe VJ, Wiste HJ, Gunter JL, Senjem ML, et al. Tau, amyloid, and cascading network failure across the Alzheimer's disease spectrum. *Cortex* 2017; 97: 143–59.
- Kantarci K, Lowe VJ, Boeve BF, Senjem ML, Tosakulwong N, Lesnick TG, et al. AV-1451 tau and beta-amyloid positron emission tomography imaging in dementia with Lewy bodies. *Annu Neurol* 2017; 81: 58–67.
- Kawas CH, Kim RC, Sonnen JA, Bullain SS, Trieu T, Corrada MM. Multiple pathologies are common and related to dementia in the oldest-old: the 90+ study. *Neurology* 2015; 85: 535–42.
- Klunk WE, Engler H, Nordberg A, Wang Y, Blomqvist G, Holt DP, et al. Imaging brain amyloid in Alzheimer's disease with Pittsburgh Compound-B. *Ann Neurol* 2004; 55: 306–19.
- Klunk WE, Koeppe RA, Price JC, Benzinger T, Devous M, Jagust W, et al. The centiloid project: standardizing quantitative amyloid plaque estimation by PET. *Alzheimer's Dement* 2015; 11: 1–15.
- Knopman DS, Lundt ES, Therneau TM, Vemuri P, Lowe VJ, Kantarci K, et al. Entorhinal cortex tau, amyloid-beta, cortical thickness and memory performance in non-demented subjects. *Brain* 2019.
- La Joie R, Ayakta N, Seeley WW, Borys E, Boxer AL, DeCarli C, et al. Multisite study of the relationships between antemortem [(11)C]PIB-PET Centiloid values and postmortem measures of Alzheimer's disease neuropathology. *Alzheimers Dement* 2019; 15: 205–16.
- Landau SM, Horng A, Fero A, Jagust WJ. Amyloid negativity in patients with clinically diagnosed Alzheimer disease and MCI. *Neurology* 2016; 86: 1377–85.
- Leal SL, Lockhart SN, Maass A, Bell RK, Jagust WJ. Subthreshold amyloid predicts tau deposition in aging. *J Neurosci* 2018; 38: 4482–9.
- Lemoine L, Gillberg PG, Svedberg M, Stepanov V, Jia Z, Huang J, et al. Comparative binding properties of the tau PET tracers

- THK5117, THK5351, PBB3, and T807 in postmortem Alzheimer brains. *Alzheimers Res Ther* 2017; 9: 96.
- Leuzy A, Savitcheva I, Chiotis K, Lilja J, Andersen P, Bogdanovic N, et al. Clinical impact of [(18)F]flutemetamol PET among memory clinic patients with an unclear diagnosis. *Eur J Nucl Med Mol Imaging* 2019; 46: 1276–86.
- Lim YY, Kalinowski P, Pietrzak RH, Laws SM, Burnham SC, Ames D, et al. Association of beta-amyloid and apolipoprotein E epsilon4 with memory decline in preclinical Alzheimer disease. *JAMA Neurol* 2018; 75: 488–94.
- Lopez OL, Becker JT, Chang Y, Klunk WE, Mathis C, Price J, et al. Amyloid deposition and brain structure as long-term predictors of MCI, dementia, and mortality. *Neurology* 2018; 90: e1920–8.
- Lowe VJ, Curran G, Fang P, Liesinger AM, Josephs KA, Parisi JE, et al. An autoradiographic evaluation of AV-1451 tau PET in dementia. *Acta Neuropathol Commun* 2016; 4: 58.
- Lowe VJ, Wiste HJ, Senjem ML, Weigand SD, Therneau TM, Boeve BF, et al. Widespread brain tau and its association with ageing, Braak stage and Alzheimer's dementia. *Brain* 2018; 141: 271–87.
- Maass A, Landau S, Baker SL, Horng A, Lockhart SN, La Joie R, et al. Comparison of multiple tau-PET measures as biomarkers in aging and Alzheimer's disease. *Neuroimage* 2017; 157: 448–63.
- Maass A, Lockhart SN, Harrison TM, Bell RK, Mellinger T, Swinnerton K, et al. Entorhinal tau pathology, episodic memory decline, and neurodegeneration in aging. *J Neurosci* 2018; 38: 530–43.
- Markesbery WR, Schmitt FA, Kryscio RJ, Davis DG, Smith CD, Wekstein DR. Neuropathologic substrate of mild cognitive impairment. *Arch Neurol* 2006; 63: 38–46.
- Marque M, Siao Tick Chong M, Anton-Fernandez A, Verwer EE, Saez-Calveras N, Meltzer AC, et al. [F-18]-AV-1451 binding correlates with postmortem neurofibrillary tangle Braak staging. *Acta Neuropathol* 2017; 134: 619–28.
- McKeith IG, Boeve BF, Dickson DW, Halliday G, Taylor JP, Weintraub D, et al. Diagnosis and management of dementia with Lewy bodies: Fourth consensus report of the DLB Consortium. *Neurology* 2017; 89: 88–100.
- McKhann G, Drachman D, Folstein M, Katzman R, Price D, Stadlan EM. Clinical diagnosis of Alzheimer's disease: report of the NINCDS-ADRDA Work Group under the auspices of Department of Health and Human Services Task Force on Alzheimer's Disease. *Neurology* 1984; 34: 939–44.
- McKhann GM, Knopman DS, Chertkow H, Hyman BT, Jack CR Jr, Kawas CH, et al. The diagnosis of dementia due to Alzheimer's disease: Recommendations from the National Institute on Aging and the Alzheimer's Association Workgroup. *Alzheimers Dement* 2011; 7: 263–9.
- Mishra S, Gordon BA, Su Y, Christensen J, Friedrichsen K, Jackson K, et al. AV-1451 PET imaging of tau pathology in preclinical Alzheimer disease: defining a summary measure. *Neuroimage* 2017; 161: 171–8.
- Murray ME, Lowe VJ, Graff-Radford NR, Liesinger AM, Cannon A, Przybelski SA, et al. Clinicopathologic and 11C-Pittsburgh compound B implications of Thal amyloid phase across the Alzheimer's disease spectrum. *Brain* 2015; 138 (Pt 5): 1370–81.
- Nelson PT, Alafuzoff I, Bigio EH, Bouras C, Braak H, Cairns NJ, et al. Correlation of Alzheimer disease neuropathologic changes with cognitive status: a review of the literature. *J Neuropathol Exp Neurol* 2012; 71: 362–81.
- Nelson PT, Dickson DW, Trojanowski JQ, Jack CR, Boyle PA, Arfanakis K, et al. Limbic-predominant age-related TDP-43 encephalopathy (LATE): consensus working group report. *Brain* 2019; 142: 1503–27.
- Nelson PT, Head E, Schmitt FA, Davis PR, Neltner JH, Jicha GA, et al. Alzheimer's disease is not “brain aging”: neuropathological, genetic, and epidemiological human studies. *Acta Neuropathol* 2011; 121: 571–87.
- Nordberg A, Carter SF, Rinne J, Drzezga A, Brooks DJ, Vandenberghe R, et al. A European multicentre PET study of fibrillar amyloid in Alzheimer's disease. *Eur J Nucl Med Mol Imaging* 2013; 40: 104–14.
- Ossenkoppele R, Jansen WJ, Rabinovici GD, Knol DL, van der Flier WM, van Berckel BN, et al. Prevalence of amyloid pet positivity in dementia syndromes: a meta-analysis. *JAMA* 2015; 313: 1939–49.
- Ossenkoppele R, Rabinovici GD, Smith R, Cho H, Schöll M, Strandberg O, et al. Discriminative accuracy of F18 flortaucipir positron emission tomography for Alzheimer disease vs other neurodegenerative disorders. *JAMA* 2018; 320: 1151–62.
- Ossenkoppele R, Schonhaut DR, Scholl M, Lockhart SN, Ayakta N, Baker SL, et al. Tau PET patterns mirror clinical and neuroanatomical variability in Alzheimer's disease. *Brain* 2016; 139 (Pt 5): 1551–67.
- Petersen RC. Mild cognitive impairment as a diagnostic entity. *J Intern Med* 2004; 256: 183–94.
- Petersen RC. How early can we diagnose Alzheimer disease (and is it sufficient)? The 2017 Wartenberg lecture. *Neurology* 2018; 91: 395–402.
- Pontecorvo MJ, Devous MD Sr, Navitsky M, Lu M, Salloway S, Schaerf FW, et al. Relationships between flortaucipir PET tau binding and amyloid burden, clinical diagnosis, age and cognition. *Brain* 2017a; 140: 748–63.
- Pontecorvo MJ, Siderowf A, Dubois B, Doraiswamy PM, Frisoni GB, Grundman M, et al. Effectiveness of florbetapir PET imaging in changing patient management. *Dement Geriatr Cogn Disord* 2017b; 44: 129–43.
- Rabinovici GD, Gatsonis C, Apgar C, Chaudhary K, Gareen I, Hanna L, et al. Association of amyloid positron emission tomography with subsequent change in clinical management among medicare beneficiaries with mild cognitive impairment or dementia. *JAMA* 2019; 321: 1286–94.
- Rabinovici GD, Jagust WJ, Furst AJ, Ogar JM, Racine CA, Mormino EC, et al. Abeta amyloid and glucose metabolism in three variants of primary progressive aphasia. *Ann Neurol* 2008; 64: 388–401.
- Rascovsky K, Hodges JR, Knopman D, Mendez MF, Kramer JH, Neuhaus J, et al. Sensitivity of revised diagnostic criteria for the behavioural variant of frontotemporal dementia. *Brain* 2011; 134 (Pt 9): 2456–77.
- Roberts RO, Geda YE, Knopman DS, Cha RH, Pankratz VS, Boeve BF, et al. The Mayo Clinic Study of Aging: design and sampling, participation, baseline measures and sample characteristics. *Neuroepidemiology* 2008; 30: 58–69.
- Schneider JA, Arvanitakis Z, Bang W, Bennett DA. Mixed brain pathologies account for most dementia cases in community-dwelling older persons. *Neurology* 2007; 69: 2197–204.
- Scholl M, Lockhart SN, Schonhaut DR, O'Neil JP, Janabi M, Ossenkoppele R, et al. PET imaging of tau deposition in the aging human brain. *Neuron* 2016; 89: 971–82.
- Schwarz CG, Gunter JL, Lowe VJ, Weigand S, Vemuri P, Senjem ML, et al. A comparison of partial volume correction techniques for measuring change in serial amyloid PET SUVR. *J Alzheimers Dis* 2019; 67: 181–95.
- Scrucca L, Fop M, Murphy TB, Raftery AE. mclust 5: clustering, classification and density estimation using gaussian finite mixture models. *R J* 2016; 8: 289–317.
- Sonnen JA, Larson EB, Crane PK, Haneuse S, Li G, Schellenberg GD, et al. Pathological correlates of dementia in a longitudinal, population-based sample of aging. *Ann Neurol* 2007; 62: 406–13.
- Sperling RA, Mormino EC, Schultz AP, Betensky RA, Papp KV, Amariglio RE, et al. The impact of amyloid-beta and tau on prospective cognitive decline in older individuals. *Ann Neurol* 2019; 85: 181–93.
- St Sauver JL, Grossardt BR, Leibson CL, Yawn BP, Melton LJ, Rocca WA. Generalizability of epidemiological findings and public health decisions: an illustration from the Rochester Epidemiology Project. *Mayo Clin Proc* 2012; 87: 151–60.

- Timmers T, Ossenkoppele R, Verfaillie SCJ, van der Weijden CWJ, Slot RER, Wesselman LMP, et al. Amyloid PET and cognitive decline in cognitively normal individuals: the SCIENCe project. *Neurobiol Aging* 2019; 79: 50–8.
- Villemagne VL, Burnham S, Bourgeat P, Brown B, Ellis KA, Salvado O, et al. Amyloid beta deposition, neurodegeneration, and cognitive decline in sporadic Alzheimer's disease: a prospective cohort study. *Lancet Neurol* 2013; 12: 357–67.
- Villemagne VL, Dore V, Bourgeat P, Cummins TL, Pejoska S, Mulligan RS, et al. The tau MeTeR scale for the generation of continuous and categorical measures of tau deposits in the brain: results from 18F-AV1451 and 18F-THK5351 tau imaging studies. *Alzheimer's Dement* 2016; 12: 244.
- Walker L, McAleese KE, Thomas AJ, Johnson M, Martin-Ruiz C, Parker C, et al. Neuropathologically mixed Alzheimer's and Lewy body disease: burden of pathological protein aggregates differs between clinical phenotypes. *Acta Neuropathol* 2015; 129: 729–48.
- Wisse LE, Butala N, Das SR, Davatzikos C, Dickerson BC, Vaishnavi SN, et al. Suspected non-AD pathology in mild cognitive impairment. *Neurobiol Aging* 2015; 36: 3152–62.
- Wolk DA, Price JC, Madeira C, Saxton JA, Snitz BE, Lopez OL, et al. Amyloid imaging in dementias with atypical presentation. *Alzheimers Dement* 2012; 8: 389–98.
- Xiong C, Jasielec MS, Weng H, Fagan AM, Benzinger TL, Head D, et al. Longitudinal relationships among biomarkers for Alzheimer disease in the Adult Children Study. *Neurology* 2016; 86: 1499–506.